IEEE Access
Multidisciplinary | Rapid Review | Open Access Journal

Received 23 March 2023, accepted 21 April 2023, date of publication 25 April 2023, date of current version 24 May 2023.

Digital Object Identifier 10.1109/ACCESS.2023.3270286

RESEARCH ARTICLE

Model Predictive Control With Disturbance Observer for Marine Diesel Engine Speed Control

HAOYU SHU[1], XUEMIN LI[1], YUFEI LIU[2], AND RUNZHI WANG[3]

[1]College of Power and Energy Engineering, Harbin Engineering University, Harbin 150001, China
[2]Beijing Jingwei Hirain Technology GmbH, Chaoyang, Beijing 100020, China
[3]School of Mechanical and Electrical Engineering, Suqian University, Suqian 223800, China

Corresponding author: Xuemin Li (lxm@hrbeu.edu.cn)

This work was supported by Harbin Engineering University, Harbin, China.

ABSTRACT The application of model predictive control (MPC) algorithm in the fixed phase control of marine diesel engine speed is studied under the premise of considering model mismatch and external disturbance. Firstly, the steady-state error problem of conventional MPC controller is solved by changing nonlinear model to incremental form. Furthermore, discrete disturbance observer (DO) is introduced in the feedback correction, which can filter out the high-frequency disturbance and reduce the requirement of algorithm on the accuracy of model. Then, considering that nonlinear MPC based on DO (DONMPC) requires a large amount of online computation, the algorithm is simplified by preliminarily converting the nonlinear model to linear model. Through analysis, the controller performance of the two models is similar. Furthermore, considering that the speed of marine diesel engine is usually set to a few fixed reference values, a linear multi-model predictive controller based on DO (DOLMMPC) with less online calculation is proposed. Finally, the designed controllers are verified by experiments. The software simulations of the designed controllers and the PID controller are carried out on the cylinder-by-cylinder mean value engine model (MVEM). It is proved that the algorithm simplification method retains the control performance of the DONMPC algorithm, and the control performance of the designed two controllers is better than the PID controller. Moreover, the DOLMMPC controller and PID controller are tested on the semi-physical simulation platform. The results demonstrate that the DOLMMPC controller can meet the computational power limit of the microprocessor in practical engineering.

INDEX TERMS Disturbance observer, marine diesel engine, model predictive control, mean value engine model, speed control.

I. INTRODUCTION

Diesel engine has become the main power source of modern marines because of its high thermal efficiency and excellent durability [1], [2], [3]. This type of engine usually operates at several specified speeds to ensure that the marine is sailing at an appropriate speed [2], [3], [4], which requires us to exert precise closed-loop control over the diesel engine speed. However, diesel engine is a kind of typical strong nonlinear system, including the nonlinear relationship between fuel injection delay and fuel rail pressure, the change of combustion characteristics caused by environmental changes, the aging of engine parts and other factors [5], [6]. In addition, the complicated sea state will also bring the diesel engine load torque drastic uncertainty change. The conventional PID controller adopts the way of off-line tuning, although it does not depend on the model parameters, and has a good control performance in the set operating condition, but when the diesel engine operating condition changes, the control performance will be greatly reduced due to the existence of complex factors such as nonlinear, time-varying and delay. The aging of engine parts will also make the calibrated parameters no longer the optimal solution, leading to the gradual deterioration of control performance over time. For a long time,

The associate editor coordinating the review of this manuscript and approving it for publication was Tao Wang.

scholars in related fields have been working on the design of a new speed controller, which can be applied to the complex diesel engine system and ensure the economic and dynamic performance of the diesel engine during operation.

Some scholars try to study an algorithm to combine with PID controller, and put forward the adaptive PID control. The real-time optimization of PID parameters is realized by parameter tuning algorithm to improve the robustness and adaptability of the controller. It mainly includes fuzzy PID controller [7], [8], PID controller which adjusts parameters based on swarm intelligent algorithm [9], [10] or neural network algorithm [11]. These have the advantage of combining the capabilities and advantages of the two algorithms. However, it should be emphasized that the performance of fuzzy PID control depends heavily on the fuzzy rules designed manually, and this is a tedious process [12]. PID algorithm based on swarm intelligent algorithm or neural network algorithm to adjust parameters faces the problem of slow convergence speed [13], [14], in many fields can not meet the real-time requirements, thus affecting the control performance. Especially in the field of diesel engine speed control, most of them can not be applied in engineering.

Others make attempt to get rid of PID controller and find a better control algorithm to replace it. Active disturbance rejection control (ADRC) is a new algorithm developed on the basis of PID. Reference [15] studies linear ADRC and nonlinear ADRC, so as to replace PID controller to cope with strong nonlinear and complex environmental disturbance of marine diesel engine. In [16], an ADRC controller based on crankshaft angle domain is further proposed. The advantage of this design is to make the controller closer to the actual control process. Reference [4] introduces the sliding mode control (SMC) into the speed control of marine diesel engine, and built a discrete SMC controller based on DO. The chattering problem of SMC algorithm is effectively reduced by the design of reaching law. However, as microprocessor technology has been iteratively upgraded, so has its computing power. At present, the new diesel engine speed controller should not only cope with the complex characteristics of the diesel engine, but also take into account the robustness, environmental adaptability and certain optimization ability.

The MPC algorithm can deal with constraint problems explicitly based on the predictive model, and it has certain robustness due to its rolling optimization of the control process. However, it does not need to explore the entire time domain and requires relatively small amount of computation unlike optimal control algorithm. Meanwhile, the contradiction between rapidity and stability of control performance can be solved by designing the objective function. Hence, MPC has developed rapidly since it came out. However, there is little literature on the application of MPC in the field of diesel engine speed control. The leading cause is that the optimization process of MPC needs iterative calculation. Although the computation is reduced compared with the global optimization, it is still difficult to meet the response requirements in the field with high real-time requirements such as diesel engine speed control. Therefore, an important research direction is how to reduce the computational load of MPC without seriously affecting its control performance [17]. In [18], predictive function control (PFC) is adopted in the path control of industrial robots. By introducing basis functions, the control input is regarded as a linear combination of selected basis functions, and the predictive output is obtained by simple calculation according to the system output under the action of each basis function obtained by offline calculation, which not only ensures the regularity of the control input but also reduces the amount of online calculation to a certain extent. Explicit model predictive control (EMPC) has been thoroughly studied in [19]. Based on the idea of parameter programming, it divided several feasible domains in the state space according to constraint conditions, and calculated the EMPC control law under each feasible domain offline. In online calculation, it only needed to query the feasible domain to select the corresponding control law. However, when the time domain length increases, the number of feasible domains increases geometrically, which requires a large amount of storage space and online search time, so it is only applicable to small-scale control [20]. In addition to these relatively mature methods, many scholars improve the computation process for their own control objects to improve the operation rate. Laguerre function was introduced in [21] to describe the control incremental signal, thus reducing the dimensions of each coefficient matrix in the optimization problem and improving the operation rate of MPC in marine dynamic positioning control. Reference [22] reduces the quadratic programming operation time of MPC in FPGA through particle swarm optimization algorithm and parallel operation based on FPGA.

In addition to the above problems, the performance of conventional MPC also depends on the accuracy of the prediction model. If the model is badly mismatched, the control performance will be greatly decreased. And the rolling optimization and feedback process are not sufficient to suppress signal fluctuations at this time. There are two common approaches to this problem. One is to use online identification as system feedback to update the prediction model [23], [24], which is a good solution for the system which is difficult to model and has low requirement on real-time, but in the field of diesel engine speed control, it is difficult to meet the real-time requirement. The other called multi-model predictive control [25], [26], which multiple prediction models are established under different operating conditions. When the algorithm is running, the corresponding prediction models of adjacent operating conditions are taken as reference for calculation. Although the control accuracy of the multi-model method is inferior to that of the online identification method, it makes up for the defects of the conventional MPC by a large margin, and does not increase the amount of extra computation basically.

Even MPC itself has the above problems, its excellent ability in dealing with multi-constraint and multi-variable problems makes it widely used in various fields. References [27], [28], [29], [30], and [31] apply MPC to intelligent vehicles, unmanned aerial vehicles, robots, motor control and other fields. In addition, MPC is also tried to be used in the control fields of engine gas path, power, torque and so on [32], [33], [34], [35]. In conclusion, the application of MPC in the field of diesel engine speed is worthy of further research.

Aiming at simplifying calculation and improving tracking performance, this manuscript attempts to design a diesel engine speed controller based on MPC algorithm which can be applied to practical engineering. In addition, a DO is introduced in the feedback to estimate the disturbance in the predictive model. DO can estimate unknown disturbance by the change of known state of the system. Its appearance aims to enhance the robustness of the control system to disturbance [36]. The disturbance mentioned here is generalized and can represent either external unknown disturbance or unknown action due to the uncertainty of the parameters of the controlled system. Therefore, the introduction of DO will reduce the dependence of MPC controller on the precise model. Firstly, the DONMPC controller are designed using nonlinear model, and the steady-state error is avoided by changing the predictive model to an incremental form. Then, considering that the nonlinear terms in the nonlinear model occupy a lot of computational resources in the prediction and solving process, the nonlinear model is preliminarily simplified to linear model. And the parameters of the linear model are updated by the system identification of the simulation model. However, although the model used for algorithm design has been simplified, the optimization solution still needs a lot of calculation. Therefore, the DOLMMPC controller which is less computative and can run in the microprocessor is further designed by changing the prediction model with time-varying parameters to one with multiple fixed parameters under different selected operating conditions, and adopting off-line calculation of coefficient matrix, the online calculation amount is greatly reduced.

The rest of this manuscript consists of the following. In the second section, some of the preparatory work is described, including the establishment of the diesel engine model, the derivation of the model formula for the algorithm design and the design of discrete DO. In the third section, the speed controller based on DONMPC and DOLMMPC is designed successively. The design process aims to gradually simplify the calculation amount of the algorithm, so as to meet the requirements of practical engineering applications. In the fourth section, the two speed controllers designed and the conventional PID controller are respectively tested by software simulation under multiple operating conditions on the cylinder-by-cylinder MVEM, and the experimental results are compared and analyzed. Meanwhile, the designed DOLMMPC controller and PID controller are tested to prove the feasibility of the designed controller in the application of the microprocessor based on the semi-physical simulation platform. Finally, the work and achievements of this research are summarized.

II. PRELIMINARIES

This section will introduce some work before the controller design, including the construction of simulation model, the derivation of some basic formulas in algorithm design and the construction of nonlinear discrete DO. Meanwhile, it also be emphasized that the basic composition of the controlled system in this manuscript is shown in Fig.1. It is a six-cylinder four-stroke turbocharged diesel engine, which is composed of turbocharger, intake and exhaust manifold, diesel engine electronic control unit (ECU), gearbox, propeller and engine body. In addition, a telegraph is connected to input the reference speed.

A. SIMULATION MODEL OF MARINE DIESEL ENGINE

The working process of diesel engine has the characteristics of separate cylinders and stages. The speed control adopts the mode of fixed phase input, and the injection interval changes with the speed change. However, in the past research on diesel engine speed control, the MVEM is mostly used, which is based on the assumption that the diesel engine working process is continuous and internal space is uniform field. It is a modeling method that completely ignores the internal working process of diesel engine and only cares about the change of macro parameters. The MVEM can neither describe the periodic fluctuation of diesel engine speed nor be used for fixed phase control. In order to better simulate the working characteristics of diesel engine, a new modeling method is proposed for the diesel engine indicating torque and pumping torque. The MVEM can be modified into the cylinder-by-cylinder MVEM by this method. The new model is more in line with the actual working characteristics of diesel engine and can be applied to fixed phase control.

Assuming that the gearbox reduction ratio is 1, the diesel engine dynamics model can be expressed as follows when the disturbance is ignored:

$$\dot{n}_e = \frac{30}{\pi}\frac{M_i - M_p - M_f - M_{load}}{J_e + J_l} \tag{1}$$

where n_e represents the diesel engine speed, M_i represents the indicated torque of the diesel engine, M_p represents the pumping torque, M_f represents frictional torque, M_{load} represents the load torque, J_e represents the equivalent moment of inertia of the diesel engine moving parts, J_l represents the moment of inertia of the propeller and the spindle system.

Let the compound torque $M_{ip} = M_i - M_p$, which represents the equivalent torque generated by cylinder pressure acting on the piston after considering the pumping torque. By analyzing the force diagram of the crank-link mechanism in Fig.2, the compound torque can be expressed as:

$$M_{ip}(t) = \sum_{j=1}^{6} \frac{\pi \sin(\phi_j + \theta_j)}{4\cos\phi_j} r d^2 p_{c,j}(t) \tag{2}$$

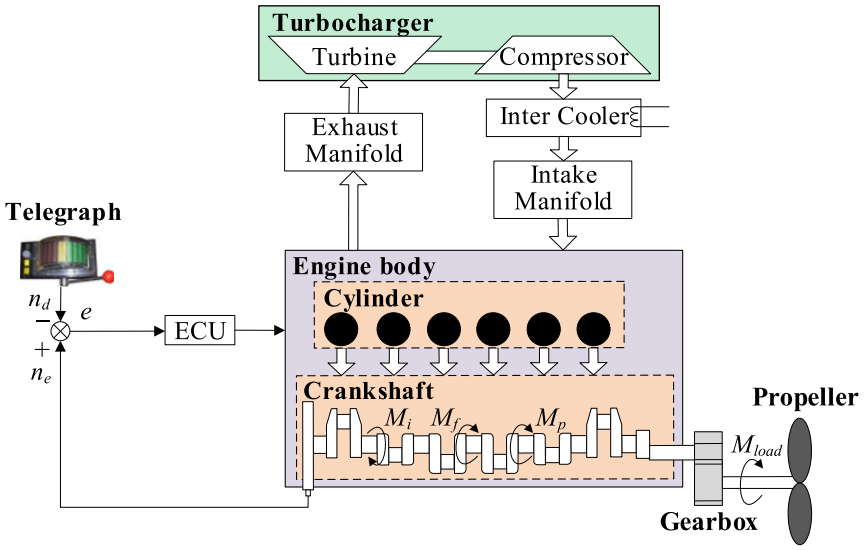

FIGURE 1. The structure of a marine diesel engine control system for propulsion.

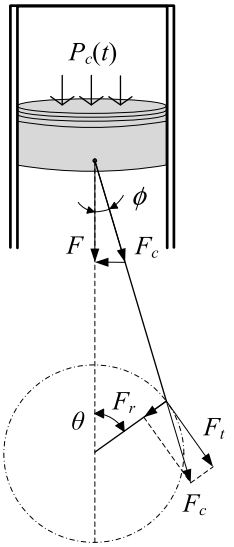

FIGURE 2. Force diagram of crank-link mechanism.

where r represents the radius of the crankshaft, d represents the diameter of the cylinder, p_c represents the cylinder pressure, ϕ represents the angle at which the linkage deviates from the center line, θ represents the angle at which the crankshaft deviates from the TDC position, the subscript j represents the cylinder number of the cylinder.

According to (2), as long as cylinder pressure p_c is calculated, compound torque M_{ip} can be obtained.

A working cycle of the cylinder is divided into five stages for cylinder pressure modeling, in order to make the calculation process more in line with the working characteristics of the diesel engine. The intake valve is opened and the exhaust valve is closed in the intake process. The cylinder pressure at this stage can be approximately considered to be equal to the pressure in the intake manifold:

$$p_{im} = p_0 + \int_0^t \frac{R_i T_{im}(t)}{V_{im}} (W_c(t) - W_{ic}(t))dt \tag{3}$$

where p_0 represents atmospheric pressure, R_i represents the intake gas constant, T_{im} represents the temperature of the gas in the intake manifold, V_{im} represents the intake manifold volume, W_c and W_{ic} represent the mass flow rate of the compressor and the mass flow rate of the gas entering the cylinder respectively.

Similarly, the cylinder pressure can be approximately considered equal to the pressure in the exhaust manifold in the exhaust process:

$$p_{em} = p_0 + \int_0^t \frac{R_e T_{em}(t)}{V_{em}} (W_{ec}(t) - W_t(t))dt \tag{4}$$

where R_e represents the exhaust gas constant, T_{em} represents gas temperature in the exhaust manifold, V_{em} represents the exhaust manifold volume, W_t and W_{ec} represent the mass flow rate of the turbine and the mass flow rate of the gas exhausting the cylinder respectively.

In (3) and (4), it is considered that the gas temperature in the intake manifold is equal to the ambient temperature, and the gas temperature in the exhaust manifold is equal to the cylinder outlet temperature. The turbocharger model is established using physical equations, and then the mass flow rate of the turbine and compressor is obtained. The modeling process is complicated, so it is not discussed in this manuscript. The mass flow of gas into and out of the cylinder is calculated according to the intake and injection quality per cycle of each cylinder and expressed as:

$$W_{ic} = \frac{\eta_v p_{im} V_d n_e}{120 R_i T_{im}} \tag{5}$$

$$W_{ec} = W_{ic} + \frac{m_f n_e N_{cyl}}{120} \tag{6}$$

where η_v represents the efficiency of the cylinder volume, V_d represents the total displacement of the diesel engine, m_f represents injection quality per cylinder per cycle, N_{cyl} represents the number of cylinders in the diesel engine.

In the scavenging process, the intake valve and the exhaust valve are opened at the same time. The general treatment method is to make the cylinder pressure transition smoothly from the exhaust stage to the intake stage by cosine interpolation. Meanwhile, the analysis shows that the pumping torque has been taken into account in the calculation of cylinder pressure in the above two stages.

The compression process of incomplete fuel combustion can be regarded as a polytropic process. The expressions of pressure and temperature are shown in (7) and (8) respectively [37]:

$$p_c(t) = p_{ivc}\left(\frac{V_{ivc}}{V(t)}\right)^{k_c} \tag{7}$$

$$T_c(t) = T_{ivc}\left(\frac{V_{ivc}}{V(t)}\right)^{k_c-1} \tag{8}$$

where p_{ivc}, V_{ivc} and T_{ivc} represent respectively the cylinder pressure, cylinder working volume, and temperature in the cylinder when the intake valve is closed, V represents real-time cylinder working volume, k_c represents polytropic index.

During the process from the start of combustion to the opening of the exhaust valve, the cylinder pressure is mainly determined by the change of the thermal energy in the cylinder. According to the first law of thermodynamics, the change of the thermal energy in the cylinder at this stage is equal to the heat released by the fuel combustion minus the energy consumed by the piston movement and heat transfer. Moreover, the cylinder volume changes very little in each simulation step, which can be approximated as a constant volume combustion process, as follows:

$$p_c(t)\dot{V}(t) = m_f q_{LHV}\eta_t\dot{x}(t) - m_{tot}c_v\dot{T}_c(t) \tag{9}$$

where q_{LHV} represents the net heating value of the fuel, fuel conversion efficiency η_t represents the proportion of the actual converted heat of the fuel combustion in the heat generated by the complete combustion of the fuel, x represents the proportion of fuel that has been combusted, m_{tot} represents the total mass of the actuating medium in the cylinder, c_v represents the specific heat at constant volume of the actuating medium in the cylinder.

Similar to indicated thermal efficiency, fuel conversion efficiency η_t is considered as a function of diesel engine speed and air-fuel ratio [38]. Assuming that η_t is a constant value within a working cycle, it can be expressed as [39]:

$$\eta_t = (k_{t1}n_e^2 + k_{t2}n_e + k_{t3})(k_{t4} - k_{t5}\lambda^{k_{t6}}) \tag{10}$$

where k_{t1}, k_{t2}, k_{t3}, k_{t4} and k_{t5} are all coefficients that need to be calibrated.

The proportion of fuel already combusted can be calculated using the single Weber combustion model as follows [40], [41]:

$$x(t) = 1 - e^{-a\left(\frac{\varphi(t)-\varphi_{soc}}{\varphi_{doc}}\right)^{m+1}} \tag{11}$$

where a and m represent the coefficients associated with the shape, φ represents crankshaft angle, φ_{soc} represents the angle of combustion, φ_{doc} represents the angle of combustion duration.

The mixed gas in the cylinder is regarded as the ideal gas, and the pressure in the cylinder can be obtained by combining the ideal gas state equation:

$$p_c(t) = \frac{m_{tot}RT_c(t)}{V(t)} \tag{12}$$

Based on the above methods, the MVEM in [42] is improved in this manuscript. The indicating torque M_i and pumping torque M_p in (1) are replaced by the compound torque M_{ip}, and the rest parts are consistent with the MVEM:

$$M_f = \frac{V_d}{4\pi}(k_{f1}n_e^2 + k_{f2}n_e + k_{f3}) \tag{13}$$

$$M_{load} = k_{Mp}\rho_w D_p^5 n_e^2 \tag{14}$$

where k_{f1}, k_{f2} and k_{f3} are the coefficients to be calibrated, k_{Mp} and D_p are the torque coefficient and diameter of the propeller, ρ_w is the density of water.

The fuel conversion efficiency was calibrated to make the cylinder-by-cylinder MVEM have the same speed response characteristics as the MVEM in [42] under the same parameters. Figure 3 shows the change of the compound torque of the diesel engine in a working cycle, and Fig.4 compares the speed response of the MVEM and the cylinder-by-cylinder MVEM with the same fuel input.

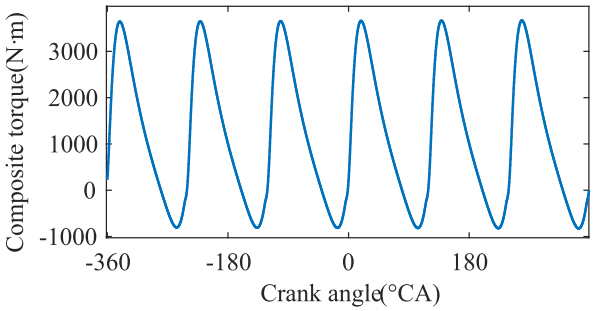

FIGURE 3. Variation of compound torque in the cylinder-by-cylinder MVEM.

B. THE MODEL FORMULA FOR ALGORITHM DESIGN

The model formula required in algorithm design will be given through simplified derivation based on the above simulation model.

By combining (1), (2), (13) and (14), (15) is derived:

$$\dot{n}_e = \psi(n_e) + g(t)m_f \tag{15}$$

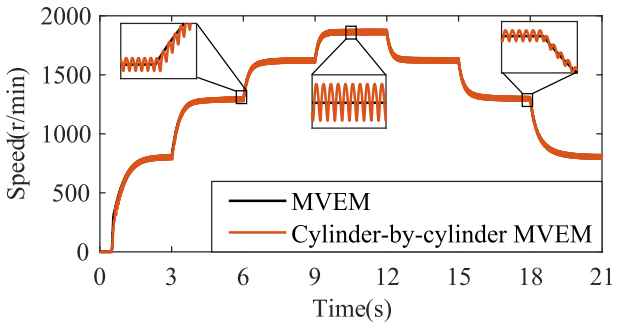

FIGURE 4. Variation of speed in the cylinder-by-cylinder MVEM.

where

$$\psi(n_e) = -\frac{30}{\pi}\frac{M_f + M_{load}}{J_e + J_l} \tag{16}$$

$$g(t) = \sum_{j=1}^{6} \frac{15rd^2 p_{c,j}(t)\sin(\phi_j + \theta_j)}{2\cos\phi_j (J_e + J_l)} \tag{17}$$

However, $g(t)$ and $\psi(n_e)$ are difficult to accurately obtain in practice. The main reason is that the exhaust temperature is not measured in practice, the fuel conversion efficiency η_t is affected by many factors, which is difficult to describe accurately, coefficient of the model of friction torque M_f and pumping torque M_p will also change in the actual operation. In addition, the complex sea state will bring many unknown disturbances, which makes the calculation of torque inaccurate. Therefore, $g(t)$ is regarded as the combination of values fluctuating within a certain range and constant g_0, and the hard part to measure of $\psi(n_e)$ and $g(t)$ and the mismatched part of the model are uniformly regarded as unknown disturbance $D(t)$ in this manuscript. Moreover, it can be seen that $\psi(n_e)$ is the quadratic function of n_e. If the actual meaning of relevant parameters in the simulation model is ignored, it can be written in the following form:

$$\dot{n}_e = A_0 n_e^2 + B_0 n_e + g_0 m_f + D(t) \tag{18}$$

where the coefficients A_0 and B_0 are determined by $\psi(n_e)$.

Let $n_e = x$, $m_f = u$, (18) is rewritten as follows:

$$\dot{x} = A_0 x^2 + B_0 x + g_0 u + D(t) \tag{19}$$

(19) was converted into discrete form in order to make designed algorithm meet the requirements of fixed phase control. Let $h(k)$ represent the interval time between two adjacent fuel injections, and use Eulerian method to discrete (19), as follows:

$$\begin{aligned} x(k+1) = {} & A_0 h(k) x^2(k) + [B_0 h(k) + 1]x(k) \\ & + g_0 h(k) u(k) + h(k) D(k) \end{aligned} \tag{20}$$

The derived (20) can be applied to the subsequent controller design.

C. DISCRETE DISTURBANCE OBSERVER

Because of $D(k)$ in (20), it cannot be directly used in the design of controller. In previous studies, $D(k)$ was usually ignored directly. However, the performance of the controller will be greatly reduced, if the model used is significantly different from the actual model. Therefore, a discrete DO is introduced in this manuscript to estimate $D(k)$, and the estimated disturbance is taken as the feedback correction. This approach also reduces the dependence of the controller on the precise model.

Suppose $D(k)$ is unknown but bounded and $D(k+1) = D(k) + h(k)p(k)$. So $p(k)$ is also bounded. With $D(k)$ as the new state variable, (20) can be expanded to the following second-order system:

$$\begin{cases} x(k+1) = x(k) + h(k)[A_0 x^2(k) + B_0 x(k) \\ \quad + g_0 u(k) + D(k)] \\ D(k+1) = D(k) + h(k)p(k) \end{cases} \tag{21}$$

Thus, the discrete DO can be written as follows:

$$\begin{cases} \widehat{z}_1(k+1) = \widehat{z}_1(k) + h(k)[A_0 x^2(k) + B_0 x(k) \\ \quad + g_0 u(k) + \widehat{z}_2(k)] \\ \widehat{z}_2(k+1) = \widehat{z}_2(k) + h(k)v(k) \end{cases} \tag{22}$$

where $\widehat{z}_1$ and $\widehat{z}_2$ are the observed values of x and D respectively, and v is the control law to be designed.

By making the difference between (22) and (21), the error system of disturbance can be obtained as follows:

$$\begin{cases} e_1(k+1) = e_1(k) + h(k)e_2(k) \\ e_2(k+1) = e_2(k) + h(k)[-p(k) + v(k)] \end{cases} \tag{23}$$

where $e_1 = \widehat{z}_1 - x$, $e_2 = \widehat{z}_2 - D$.

The disturbance can be estimated by designing the control law v so that both e_1 and e_2 of the error system (23) are convergent.

The following control law is proposed in [4]:

$$u = -\lambda e_2(k) + \mathrm{fhan}(\widehat{z}_1, c\widehat{z}_2, r_0, k_h h(k))$$

$$\begin{cases} d = r_0 h_0 \\ d_0 = h_0 d \\ y = \widehat{z}_1 + h_0 c\widehat{z}_2 \\ a_0 = \sqrt{d^2 + 8r_0|y|} \\ a = \begin{cases} c\widehat{z}_2 + \frac{a_0 - d}{2} sign(y), & |y| > d_0 \\ c\widehat{z}_2 + \frac{y}{h_0}, & |y| \le d_0 \end{cases} \\ fhan(\widehat{z}_1, c\widehat{z}_2, r_0, h_0) = -\begin{cases} r_0 sign(a), & |a| > d \\ r_0 \frac{a}{d}, & |a| \le d \end{cases} \end{cases} \tag{24}$$

where λ, h_0, r_0 and c are the coefficients to be designed, r_0 is the gain of the controlled variable, c is the damping factor. And the assumption of $e_2(k) \approx (e_1(k) - e_1(k-1))/h(k-1)$ is made to calculate approximately due to e_2 cannot be measured.

The control law (24) is improved based on the discrete sliding mode control law in [43]. It inherits the advantages of

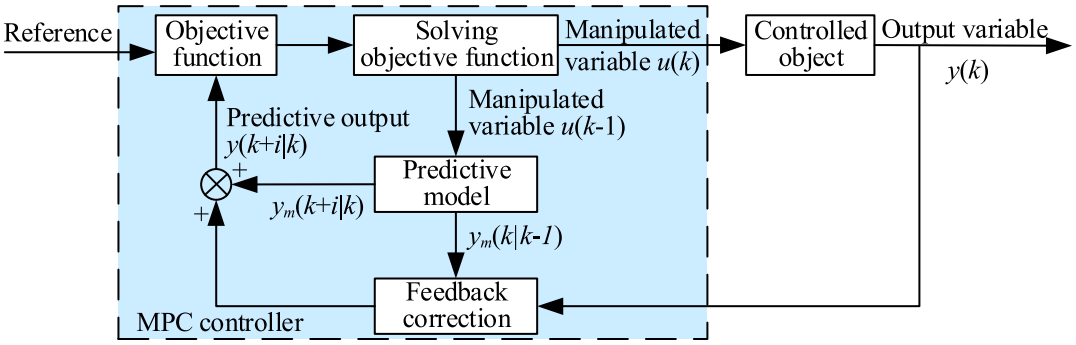

FIGURE 5. Variation of compound torque in the cylinder-by-cylinder MVEM.

the original control law, which can suppress any disturbance smaller than $(1-\frac{1}{c^2})r_0$ and converge to the origin in finite time. Moreover, chattering can be well eliminated in discrete systems by designing the ratio of h_0 to the control step size. In addition, the [4] innovatively introduced the $-\lambda e_2(k)$ term, which improved the problem that the convergence rate of the original control law was slow in the early stage.

The control law (24) is applied to obtain the following discrete DO:

$$\begin{cases} \widehat{z}_1(k+1) = \widehat{z}_1(k) + h(k)[A_0x^2(k) + B_0x(k) \\ +g_0u(k) + \widehat{z}_2(k)] \\ \widehat{z}_2(k+1) = \widehat{z}_2(k) + h(k)[-\lambda e_2(k) \\ +\text{fhan}(e_1(k), ce_2(k), r_0, k_hh(k))] \end{cases} \tag{25}$$

where $h_0 = k_hh(k)$. h_0 is called "filter factor" in reference [44], which can play a good role in suppressing chattering with proper setting. The author of [44] points out that the filtering performance is mainly determined by the ratio of h_0 to the control step size. Therefore, the introduction of k_h can ensure the filtering performance in fixed phase control.

III. DESIGN OF CONTROLLER

MPC is a prospective control method different from the control algorithm based on past and present errors. The basic structure of the MPC controller is shown in Fig.5.

A. NONLINEAR MODEL PREDICTIVE CONTROLLER

The conventional MPC controller is prone to steady-state error. In this sub-section, the causes of steady-state error will be analyzed and a DONMPC controller with better performance will be designed based on a nonlinear model.

The prediction model requires all parameters to be known, so the unknown disturbance is removed from (20) and the following prediction model is obtained:

$$\begin{aligned} x(k+1) = A_0h(k)x^2(k) + [B_0h(k)+1]x(k) \\ + g_0h(k)u(k) \end{aligned} \tag{26}$$

Considering the feedback correction, the prediction error of time $k-1$ is defined as:

$$e_p(k) = x(k) - x_m(k|k-1) \tag{27}$$

where $x_m(k|k-1)$ is the output of the system at time $k-1$, which is directly predicted according to the prediction model (26) without considering the feedback correction. The prediction error is mainly caused by the mismatch of part $h(k-1)D(k-1)$ of the prediction model.

The following assumptions are given before designing the MPC controller:

Assumption 1: The step size is constant in the predictive horizon.

Assumption 2: The unknown disturbance of the system is consistent with that of the previous time in the predictive horizon, that is, $e_p(k)$ is unchanged in the predictive horizon.

Suppose that N_{st} represents the number of strokes of the diesel engine, and it can be seen that the step size of (26) changes with the speed of the diesel engine, that is, $h(k) = 60N_{st}/(2x(k)N_{cyl})$. However, open loop control is usually adopted before the diesel engine reaches idle speed to increase the speed rapidly, and then the speed is closed loop control. At this time, the speed change between the last two working cylinders is small relative to the output speed, so the change of the last two step sizes is small. Meanwhile, the unknown disturbance $e_p(k)$ mainly consists of the mismatched part of the model which is also a function of $x(k)$, and the control horizon which is executed in practice is usually smaller than the predictive horizon. Therefore, assumption 1 and assumption 2 can greatly simplify the calculation process base on the premise of introducing only a small calculation error.

The conventional MPC controller uses the previous prediction error for feedback correction. Based on the above two assumptions, the predictive output at time k is:

$$\begin{aligned} \mathbf{X}_p(k) = A_0h(k)\mathbf{X}^2(k) + [B_0h(k)+1]\mathbf{X}(k) \\ + g_0h(k)\mathbf{U}_p(k) + \mathbf{I}\eta_e e_p(k) \end{aligned} \tag{28}$$

where $\mathbf{X}_p(k) = [x(k+1|k)x(k+2|k)\cdots x(k+p|k)]^T_{1\times p}$, $\mathbf{X}(k) = [x(k)x(k+1|k)\cdots x(k+p-1|k)]^T_{1\times p}$, $\mathbf{X}^2(k) = [x^2(k)x^2(k+1|k)\cdots x^2(k+p-1|k)]^T_{1\times p}$, $\mathbf{U}_p(k) = [u(k)u(k+1)\cdots u(k+m-1)\cdots u(k+m-1)]^T_{1\times p}$, $\mathbf{I} = [1\ 1\ \cdots\ 1]^T_{1\times p}$ and $\eta_e \in (0,1)$ is the feedback correction coefficient of the prediction error, p and m are the predictive horizon and control horizon respectively.

The research of diesel engine speed control requires that the system can follow the reference speed well, but the control variable should not change dramatically. The objective function is designed as follows:

$$J(k) = \sum_{i=1}^{p} [\gamma_y(i)(x(k+i|k) - x_r(k+i))]^2 + \sum_{i=1}^{m} [\gamma_u(i)(u(k+i-1) - u_{act}(k-1))]^2 \quad (29)$$

where $u_{act}(k-1)$ is the control variable actually executed at time $k-1$. $\gamma_y(i),\ i = 1, 2, \ldots, p$ and $\gamma_u(i),\ i = 1, 2, \ldots, m$ are the weight coefficients. $x_r(k+i),\ i = 1, 2, \ldots, p$ is the reference output in the current predictive horizon.

The speed control of marine diesel engine is mainly limited by the maximum fuel injection quantity and the fuel injection quantity set according to other state parameters, so the constraint can be described as:

$$0 \le u \le u_{lmt}(t),\ u_{lmt}(t) \le u_{\max}(t) \quad (30)$$

where $u_{lmt}(t)$ is the real-time injection quality limit determined by relevant state parameters, and $u_{\max}(t)$ is the maximum injection quality limit.

The optimal control sequence can be obtained by solving so that $u(k+i-1)$ is minimized.

Next, the steady-state error of conventional MPC controller is analyzed. The formula of the predictive output under the conventional feedback correction method is showed in (28). If the system has reached steady state at time k, the reference value of the output variable satisfies $x_r(k) = x_r(k+i),\ i = 1, 2, \ldots, p$. According to (28), there may be a large deviation between $x(k)$ and $x_r(k)$ at this time, but $u(k) = u_{act}(k-1)$ can make $x(k+i|k), i = 2, 3, \ldots, p$ close to $x_r(k)$. So $u(k) = u_{act}(k-1)$ may become the optimal solution at the current moment and be executed due to $\sum_{i=1}^{m} [\gamma_u(i)(u(k+i-1) - u_{act}(k-1))]^2 = 0$ in the objective function $J(k)$, and the optimal solution obtained is not completely accurate. Similarly, the next step of rolling optimization will still get the same solution. As a result, there is always a fixed steady-state error between the actual system output $x(k)$ and $x_r(k)$. This problem is even worse when $m > 1$. Since the $\sum_{i=1}^{p} [\gamma_y(i)(x(k+i|k) - x_r(k+i))]^2$ term in the objective function $J(k)$ has nothing to do with $u(k)$, so it only needs to meet the condition that if $u(k) = u_{act}(k-1)$, the predictive output $x(k+1|k)$ can be close to $x_r(k)$. Then, even if the deviation between $x(k+i|k), i = 2, 3, \ldots, p$ and $x_r(k)$ is large, the optimal solution obtained in the optimization solution may be $u_{act}(k-1)$, thus leading to the steady-state error. The steady-state error might be larger than if $m = 1$.

The prediction model (26) is converted into the following incremental form in order to solve the above problems:

$$\Delta x(k+1) = A_0 h(k) \Delta^2 x(k) + [B_0 h(k) + 1]\Delta x(k) + g_0 h(k) \Delta u(k) \quad (31)$$

where $\Delta x^2(k) = x^2(k) - x^2(k-1)$, $\Delta x(k) = x(k) - x(k-1)$ and $\Delta u(k) = u(k) - u(k-1)$.

The output at time $k+1$ is predicted at time k by introducing $e_p(k)$ in (31). $x(k+1|k)$ is represented as:

$$x(k+1|k) = x(k) + A_0 h(k) \Delta x^2(k) + [B_0 h(k) + 1]\Delta x(k) + g_0 h(k) \Delta u(k) + \eta_e e_p(k) \quad (32)$$

In view of the above improvement measures, the steady-state error problem is reanalyzed. If the steady state is reached, there are $\Delta x^2(k) = 0$, $\Delta x(k) = 0$ and $\Delta u(k) = 0$ at any time, so $x(k+1|k) = x(k) + \eta_e e_p(k)$. In this case, it can be seen from the definition of (27) that $e_p(k) = 0$, and the premise that $x(k+1|k)$ approaches $x_r(k)$ is that $x(k)$ approaches $x_r(k)$. Therefore, the steady-state error can be significantly reduced by using the prediction model (31) to design MPC controller.

In addition, we know that $e_p(k) = h(k-1)D(k-1)$ under ideal circumstances from the definition of $e_p(k)$ in (27). According to the actual situation, the system disturbance may also appear the transient disturbance with rapid change in addition to the slow disturbance caused by the model mismatch. Moreover, the measurement of $x(k)$ will also contain noise in practice, and there will be differences in each cycle of the diesel engine, which will be included in $e_p(k)$. The accuracy of the prediction output will be seriously affected, and the control performance will be worse, if the above unnecessary factors are introduced into the feedback correction. That's why η_e is usually less than 1. Meanwhile, it can be seen from the above that the DO can not only estimate the disturbance, but also filter the transient disturbance to a certain extent. Therefore, the DO (25) is used in this manuscript to observe the disturbance, so as to replace $e_p(k)$ for feedback correction and further improve the control performance of the MPC controller.

According to assumption 1 and assumption 2, the equation of prediction output based on the incremental prediction model which the observation error is introduced is:

$$\mathbf{X}_p(k) = \mathbf{X}(k) + A_0 h(k) \Delta \mathbf{X}^2(k) + [B_0 h(k) + 1]\Delta \mathbf{X}(k) + g_0 h(k) \Delta \mathbf{U}_p(k) + \mathbf{I}_k h(k) \Delta \widehat{D}(k) \quad (33)$$

where $\mathbf{I}_k = [10 \cdots 0]^T_{1\times p}$.

The objective function is converted into the following form:

$$J(k) = \sum_{i=1}^{p} [\gamma_y(i)(x(k+i|k) - x_r(k+i))]^2 + \sum_{i=1}^{m} [\gamma_u(i)\Delta u(k+i-1)]^2 \quad (34)$$

The limit of control increment in optimization solution is converted into the following form:

$$-u_{act}(k-1) \le \mathbf{S}_{lmt} \Delta \mathbf{U}(k) \le u_{lmt}(t) - u_{act}(k-1) \quad (35)$$

where $\Delta\mathbf{U}(k) = [\Delta u(k)\Delta u(k+1)\cdots\Delta u(k+m-1)]^T_{1\times m}$, $\mathbf{S}_{lmt} = \begin{bmatrix} 1 & 0 & \cdots & 0 \\ 1 & 1 & \ddots & \vdots \\ \vdots & \vdots & \ddots & 0 \\ 1 & 1 & \cdots & 1 \end{bmatrix}_{m\times m}$.

Compared with the conventional nonlinear MPC controller, the DONMPC controller designed in this manuscript can not only avoid the steady-state error, but also play a certain role in filtering the transient disturbance and noise. Meanwhile, the introduction of DO reduces the requirement of the controller to the accuracy of the prediction model.

B. LINEAR MULTIPLE MODEL PREDICTIVE CONTROLLER

According to the above, iterative calculation is needed repeatedly in the process of calculating predictive output and optimizing solution. The heavy computing load prevents the DONMPC controller from being used in real microprocessor. Therefore, this sub-section will simplify the DONMPC controller and ensure control performance in the process of gradual simplification.

The nonlinear term $A_0h(k)x^2(k)$ is an important reason to increase the amount of computation in the iterative calculation, so it is first considered to ignore this term and converted the nonlinear prediction model into linear.

Ignoring the nonlinear term, (20) is simplified as:

$$x(k+1) = [Bh(k)+1]x(k) + Ch(k)u(k) + h(k)D_L(k) \tag{36}$$

where B and C are the parameters of the linear system, which can be obtained through the model identification, and D_L represents the new disturbance after using the linear model.

Convert (36) into the incremental form:

$$\begin{aligned}\Delta x(k+1) = {} & [Bh(k)+1]\Delta x(k) + Ch(k)\Delta u(k) \\ & + h(k)\Delta D_L(k)\end{aligned} \tag{37}$$

Ignoring the disturbance terms of linear model (36) and (37), the prediction model (38) and incremental prediction model (39) can be obtained:

$$x(k+1) = [Bh(k)+1]x(k) + Ch(k)u(k) \tag{38}$$

$$\Delta x(k+1) = [Bh(k)+1]\Delta x(k) + Ch(k)\Delta u(k) \tag{39}$$

Comparing (20) and (36), it can be seen that there will always be a state x_0 such that $B = A_0x_0 + B_0$. When the same system output $x(k)$ at the current time is adopted, the difference between the nonlinear prediction model (26) and the linear prediction model (38) for the prediction output at the next time is:

$$\begin{aligned}e_0 &= A_0h(k)x^2(k) + [B_0 - B]h(k)x(k) + (g_0 - C)h(k)u(k) \\ &= A_0[x(k) - x_0]h(k)x(k) + (g_0 - C)h(k)u(k)\end{aligned} \tag{40}$$

The difference between (31) and (39) can be expressed as:

$$\begin{aligned}e_1 &= A_0h(k)\Delta x^2(k) - A_0x_0h(k)\Delta x(k) + (g_0 - C)h(k)\Delta u(k) \\ &= A_0[x(k) - x_0]h(k)x(k) - A_0[x(k-1) - x_0]h(k)x(k-1) \\ &\quad + (g_0 - C)h(k)\Delta u(k)\end{aligned} \tag{41}$$

Assuming $C \approx g_0$, then the value of e_0 is mainly determined by $A_0[x(k) - x_0]h(k)x(k)$, and the error increases with the increase of $x(k)$ or $|x(k) - x_0|$. However, e_1 is equivalent to introducing the feedback correction term $A_0[x(k-1) - x_0]h(k)x(k-1)$ by comparison with e_0. Although there is an extra deviation $-A_0[x(k-1) - x_0]h(k)x(k-1)$ when $x(k) = x_0$, the deviation between $x(k)$ and $x(k-1)$ is small according to the actual operating condition of diesel engine. So $x(k-1)$ is not going to deviate very much from x_0. When the deviation between $x(k)$ and x_0 is large under normal operating condition, the feedback correction term will compensate the $A_0[x(k) - x_0]h(k)x(k)$ term to a large extent due to the small difference between $x(k)$ and $x(k-1)$. In addition, it can be seen from the working characteristics of diesel engine that $\Delta u(k)$ is usually small and far smaller than $u(k)$. e_1 will not be too large, even if there is a large deviation between the identified C and g_0. Therefore, the incremental linear prediction model can still have similar prediction performance as the nonlinear prediction model without considering the disturbance. It can be seen from the above analysis that the incremental prediction model can also reduce the steady-state error.

In order to further simplify the computation, a linear discrete DO in the form of (42) is designed according to the method mentioned above.

$$\begin{cases} \widehat{z}_1(k+1) = \widehat{z}_1(k) + h(k)(Bx(k) + Cu(k) \\ \quad +\widehat{z}_2(k)) \\ \widehat{z}_2(k+1) = \widehat{z}_2(k) + h(k)[-\lambda e_2(k) \\ \quad +fhan(e_1(k), ce_2(k), r_0, k_hh(k))] \end{cases} \tag{42}$$

The prediction accuracy of the prediction model (39) can be further improved by introducing the new observed value $\widehat{D}_L(k)$ of the linear discrete DO. And then following prediction equation can be obtained based on (39):

$$\begin{aligned}\mathbf{X}_p(k) = {} & \mathbf{X}(k) + [Bh(k)+1]\Delta\mathbf{X}(k) + Ch(k)\Delta\mathbf{U}_p(k) \\ & + \mathbf{I}_kh(k)\Delta\widehat{D}_L(k)\end{aligned} \tag{43}$$

However, although the use of linear prediction model greatly reduces the amount of computation, the online optimization solution still needs a lot of time. The ECU of marine diesel engine pays more attention to the function of related peripherals and has limited computing capacity. Meanwhile, it needs to perform all the control tasks, so it is difficult to meet the needs of online optimization solution. The control interval $h(k)$ at the rated speed is about 13ms for the six-cylinder four-stroke diesel engine with a rated speed of 1500 r/min, and rail pressure control, signal monitoring, data transmission and other work must be performed during the

control interval. Therefore, the research of applying MPC algorithm to diesel engine control mostly stays in the software simulation stage or only carries out calculation of MPC on the rapid control prototype which is used for laboratory test with high operation speed. The following will combine the characteristics of marine diesel engine speed control, and further simplify the MPC controller based on the linear prediction model, so as to realize the operation in the ECU.

According to (43), the predictive output is a linear function of control increment in control horizon. Let $\mathbf{D}_j = \sum_{i=1}^{j} [Bh(k)+1]^{i-1} Ch(k)$, and then the prediction output equation of the following form can be obtained by expanding the iterated terms in (43):

$$\mathbf{X}_P(k) = \mathbf{I}x(k) + \mathbf{S}_x(k)\Delta x(k) + \mathbf{S}_u(k)\Delta\mathbf{U}_P(k) + \mathbf{S}_d(k)\Delta\widehat{D}_L(k) \tag{44}$$

where

$$\mathbf{S}_x(k) = [Bh(k)+1\sum_{i=1}^{2}[Bh(k)+1]^i \cdots \sum_{i=1}^{p}[Bh(k)+1]^i]^T_{1\times p},$$

$$\mathbf{S}_d(k) = h(k)[1\sum_{i=1}^{2}[Bh(k)+1]^{i-1} \cdots \sum_{i=1}^{p}[Bh(k)+1]^{i-1}]^T_{1\times p}$$

and

$$\mathbf{S}_u(k) = \begin{bmatrix} \mathbf{D}_1 & 0 & 0 & \cdots & 0 \\ \mathbf{D}_2 & \mathbf{D}_1 & 0 & \cdots & 0 \\ \vdots & \vdots & \vdots & \ddots & \vdots \\ \mathbf{D}_m & \mathbf{D}_{m-1} & \cdots & \cdots & \mathbf{D}_1 \\ \vdots & \vdots & \vdots & \vdots & \vdots \\ \mathbf{D}_p & \mathbf{D}_{p-1} & \cdots & \cdots & \mathbf{D}_{p-m+1} \end{bmatrix}_{p\times m}.$$

The objective function (34) can be converted into the following matrix form:

$$J(k) = \left\|\mathbf{\Gamma}_y[\mathbf{X}_P(k) - \mathbf{X}_R(k)]\right\|^2 + \|\mathbf{\Gamma}_u\Delta\mathbf{U}(k)\|^2 \tag{45}$$

where $\mathbf{\Gamma}_y = \mathrm{diag}[\gamma_y(1), \gamma_y(2), \ldots, \gamma_y(p)]$ and $\mathbf{\Gamma}_u = \mathrm{diag}[\gamma_u(1), \gamma_u(2), \ldots, \gamma_u(m)]$ are the weighted matrix.

It can be seen from (30) that the constraints in the speed control of marine diesel engine mainly consist of the maximum fuel injection quantity constraint which changes with the status parameters of the diesel engine in real time and the non-negative fuel injection quantity constraint. The control output rarely exceeds the limit in the case of normal operation and reasonable controller parameters. Therefore, the limit is usually executed when the control output exceeds the limit. The constraints are also treated in the same way in this manuscript, that constraints are not considered in the calculation of MPC output. In this way, the minimum value of the objective function $J(k)$ with respect to the control increment $\Delta\mathbf{U}(k)$ can be obtained by partial derivative:

$$\frac{\partial J(k)}{\partial\Delta\mathbf{U}(k)} = 2\mathbf{S}_u^T(k)\mathbf{\Gamma}_y^T\mathbf{\Gamma}_y(\mathbf{S}_x(k)\Delta x(k) + \mathbf{I}x(k) + \mathbf{S}_d(k)\Delta\widehat{D}(k) - \mathbf{X}_R(k)) + 2(\mathbf{S}_u^T(k)\Gamma_y^T\mathbf{\Gamma}_y\mathbf{S}_u(k) + \mathbf{\Gamma}_u^T\mathbf{\Gamma}_u)\Delta\mathbf{U}(k) \tag{46}$$

When $\frac{\partial J(k)}{\partial\Delta\mathbf{U}(k)} = 0$, the control increment $\Delta\mathbf{U}$ can be obtained:

$$\Delta\mathbf{U}(k) = (\mathbf{S}_u^T(k)\mathbf{\Gamma}_y^T\mathbf{\Gamma}_y\mathbf{S}_u(k) + \mathbf{\Gamma}_u^T\mathbf{\Gamma}_u)^{-1}\mathbf{S}_u^T(k)\mathbf{\Gamma}_y^T\mathbf{\Gamma}_y\mathbf{E}_p(k) \tag{47}$$

where

$$\mathbf{E}_p(k) = \mathbf{X}_R(k) - \mathbf{S}_x(k)\Delta x(k) - \mathbf{I}x(k) - \mathbf{S}_D(k)\Delta\widehat{D}_L(k) \tag{48}$$

Thus, the MPC controller can explicitly calculate the control increment if constraints are not taken into account. As can be seen that the calculation amount of (47) is mainly determined by the coefficient matrix $\mathbf{S}_x(k)$, $\mathbf{S}_u(k)$ and $\mathbf{S}_d(k)$.

Because marine diesel engine is different from vehicle diesel engine, it mainly works under several reference speeds. It usually switches rapidly according to the set acceleration when switching between adjacent reference speeds, and the intermediate transition operating condition exists for a short time. This manuscript proposes a DOLMMPC controller, which simplifies the time-varying prediction model into several fixed prediction models based on above characteristics. It can maintain the control performance and further reduce the calculation amount at the same time. The principle of designed DOLMMPC controller is referred to Fig.6.

As can be seen from Fig.6, the parameters B and C of prediction model should be obtained first, and select the predictive horizon and control horizon during initialization. Then, the coefficient matrix $\mathbf{S}_{u,i}$, $\mathbf{S}_{x,i}$ and $\mathbf{S}_{D,i}$, $i = 1, 2, \ldots, n$, are calculated offline, where n is the number of reference speed. In online calculation, the coefficient matrix is selected according to the output speed, and then the control increment is calculated according to (47). The selection method of the coefficient matrix is to switch between the midpoints of the two adjacent reference speed. Since the midpoint is in the acceleration or deceleration stage, the difference between the predicted output speed and the reference speed at this stage is mainly determined by the difference between the output speed and the reference speed. And the difference between the output speed and the reference speed at this time is large, so the change of the calculation step size has little influence. Therefore, the method of simplifying the time-varying parameter prediction model into a multi-parameter fixed prediction model greatly reduces the calculation time of the model prediction controller.

IV. EXPERIMENT AND ANALYSIS

According to the above analysis, when the observation effect of the DO is good, the control performance of the two MPC controllers designed should be similar due to the simple and rare constraints in the diesel engine speed control and the use of the incremental linear prediction model. In this section, the control performance of the two MPC controller and PID controller is firstly compared to prove the excellence of the designed controller by software simulation. Meanwhile, it is proved that the simplification of the algorithm does

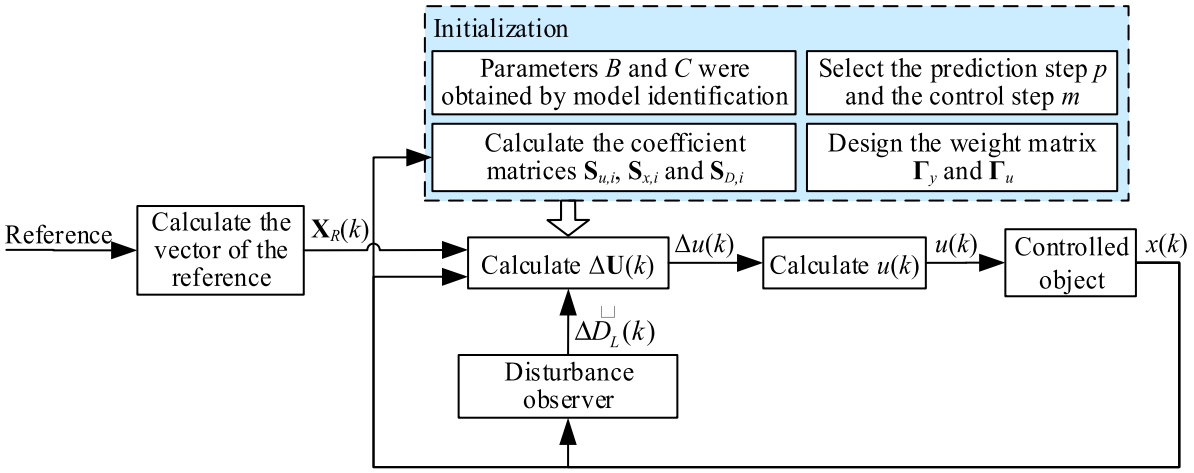

FIGURE 6. The principle of DOLMMPC controller.

not cost the loss of control performance seriously. Then, the DOLMMPC controller is verified on the semi-physical simulation platform, and the comparison and analysis with the PID controller prove that the DOLMMPC controller designed in this manuscript can run in the microprocessor. Considering the complexity of the diesel engine system, all controllers are a single set of parameters in the experiment in order to make the comparison of control effects of controllers more persuasive.

A. SOFTWARE SIMULATION AND ANALYSIS

Since the disturbance is not measurable in actual operation, it is impossible to give a comparison between the observed disturbance and the actual disturbance. Even though the external interference is known during simulation, the model mismatch is still difficult to determine. Therefore, the observation performance of disturbance can only be roughly analyzed. In contrast, we pay more attention to the convergence rate of the disturbance. Therefore, this manuscript only adopts the form of software simulation for the verification of DO. At the same time, this sub-section will conduct software simulation verification for the three model prediction controllers designed above, and make a comparative analysis with PID controller.

1) SIMULATION AND ANALYSIS OF DISCRETE DISTURBANCE OBSERVER BASED ON NONLINEAR MODEL

In order to simulate the mismatch of the model, although the parameters of the simulation model are known during the simulation, the controller parameters are only selected with approximate values, so that there is a certain deviation between disturbance observer and the diesel engine model, and the constant g_0 will also have a deviation from the time variable $g(t)$ of the model. All deviations are regarded as disturbances, and the observation effect can be seen in Fig.7.

As can be seen from the Fig.7, in the acceleration and deceleration operating conditions, the output speed and relevant state parameters of the diesel engine change slowly due to the slope limitation, so the observed speed follows well, and the observed disturbance changes are also relatively stable. The fluctuation of observed disturbance is mainly caused by the white noise added to the model during simulation. In the starting stage, the DO starts to operate when the speed reaches 300r/min for the first time. The observed speed is set to the same value as the output speed during the first operation in order to avoid excessive overshoot, so the observed disturbance calculated for the first time is 0. After that, the DO starts to work normally and gradually converges. The convergence process is relatively stable and no fluctuation. Because the DO mainly plays a compensatory role here, if the convergence speed is too fast, it is likely to produce fluctuation in some operating conditions, which worsens the control performance. At the moment of 2.5 seconds, the first loading is similar to the actual closing of the gear box. It can be seen that the observed disturbance decreases from the positive value to the negative value at this time. The change rate of the observed disturbance meets the requirements and no fluctuation. In addition, the observed speed converges to the output speed at a slower rate during loading. The reason is that if the DO pursues the convergence performance of the speed excessively, it is easy to lead to the overshoot of the observed disturbance. Moreover, even if the observation error e_2 of the disturbance is large, its convergence rate will be slow as the observation error e_1 of the speed gradually decreases. Although both converges at the same time in the end, e_2 will keep a large deviation in the convergence process, thus affecting the speed control performance. Therefore, when selecting the parameters of the DO, the performance of the observed disturbance should be given priority. This phenomenon is obvious in the load mutation operating condition. In the load mutation operating condition, the DO converges within 1 second, and there is a large error between the observed speed and the output speed in the process of convergence, while the observed

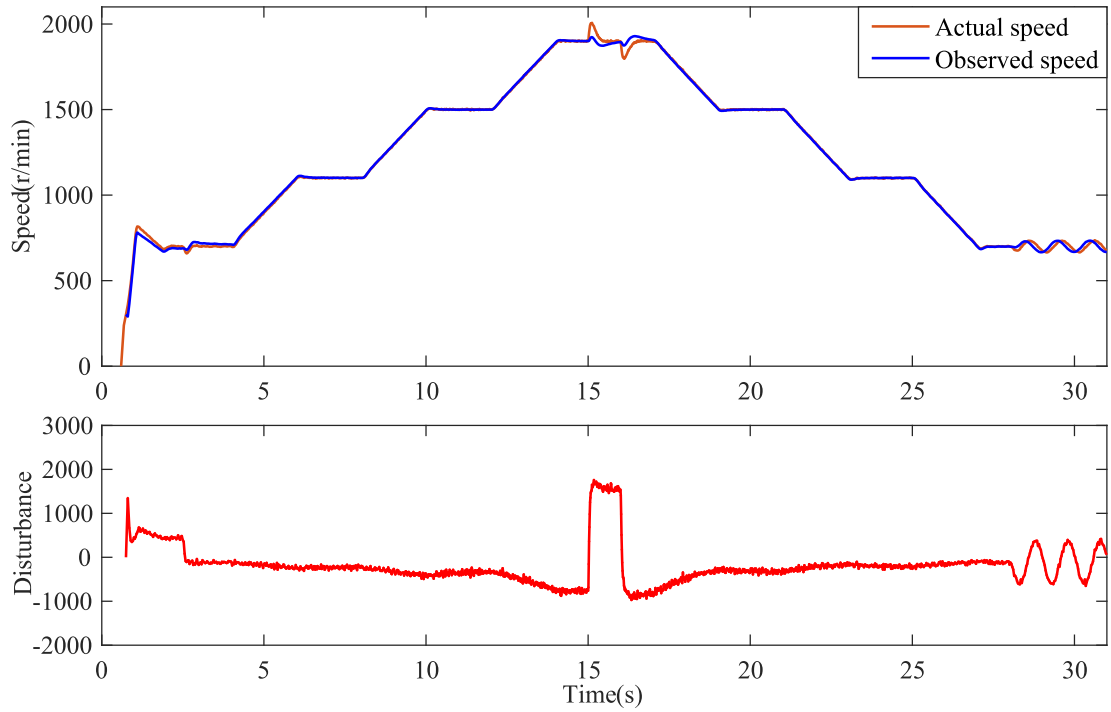

FIGURE 7. Observation effect of DO based on nonlinear model.

disturbance soon reaches stability. The disturbance observed above is more beneficial to improve the performance of the controller. In periodic load operating condition, the observed speed always keeps a certain deviation from the output speed. However, it can be seen that the observed disturbance has the same variation trend as the added disturbance, but with a slight delay by comparing the variation trend and fluctuation period of the output speed and the observed speed.

In general, when selecting the parameters of the DO, the convergence performance of the observed speed is not the target, but the convergence performance of the disturbance should prevail. In the transient operating condition of diesel engine, the DO with excellent performance should not only ensure the good convergence rate, but also avoid the fluctuation when the disturbance changes greatly.

2) SIMULATION AND ANALYSIS OF DISCRETE DISTURBANCE OBSERVER BASED ON LINEAR MODEL

The same simulation operating conditions and disturbance configuration are used for the DO based on linear model. Figure 8 shows the observation effect after the selection of new DO parameters. By comparison with Fig.7, it can be seen that the two DOs have similar observation effects on speed, and the variation trend of observed disturbance is basically the same. However, the observed disturbance values which use the two models are different due to the large difference in model mismatch between the two models.

In the acceleration and deceleration operating conditions, it can be seen that the two DOs have similar observation tracks of disturbance. However, the DO based on nonlinear model has better following performance. The observed speed of the DO based on the linear model slowly deviates from the output speed as the speed increase. This phenomenon is mainly due to the use of linear terms in the linear model instead of the original nonlinear terms, it is more likely to appear model mismatch when the diesel engine speed changes. However, the observation effect of disturbance is better at this time, and the observed speed eventually converges to the output speed. In the starting operating condition, the DO still maintains good convergence process after starting work, and there is no fluctuation. The observed speed converges more slowly at this time by comparing with the DO based-on a nonlinear model. But it can be seen that the observed disturbance at this stage is basically close to the actual disturbance by comparing the variation trend of the observed speed and the output speed. In the first loading, the observed speed still keeps a certain deviation from the output speed. And the observed speed is also close to the output speed, when the observed disturbance is reduced to the actual disturbance. Therefore, it can be seen that the observed speed maintains a good follow effect for output speed after loading. However, the disturbance observation trajectories of the two DOs are similar.

It can be seen from the above that when the parameters of the DO are selected, the following effect of the observed

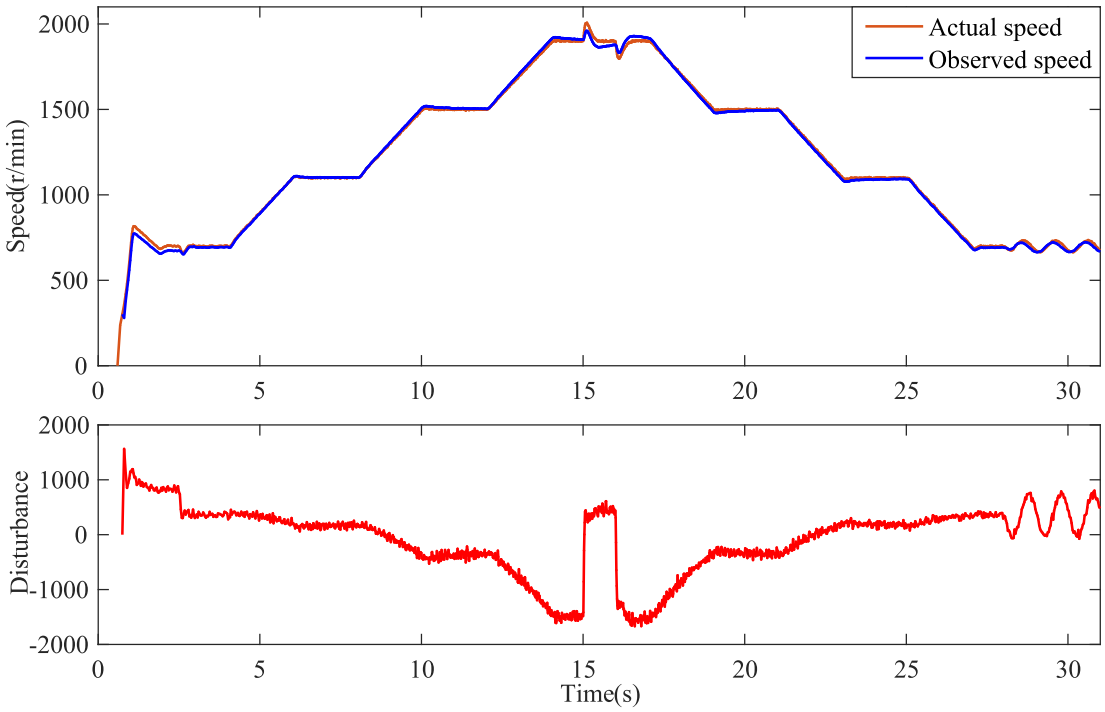

FIGURE 8. Observation effect of DO based on linear model.

speed is not the main one, but the following effect of the observed disturbance shall prevail. In the transient operating condition of diesel engine, a good DO should not only ensure rapid following speed, but also avoid the fluctuation when the disturbance changes greatly. Therefore, the DO based on linear model designed in this study- can meet the performance requirements.

3) SIMULATION AND ANALYSIS OF MODEL PREDICTION CONTROLLER

In this sub-section, the DONMPC controller and DOLMMPC controller are simulated respectively. The DO used by the DONMPC controller is the DO based on the nonlinear model. The DO used by DOLMMPC controller is the DO based on the linear model. Both DO and MPC controller use the same model parameters.

The same predictive horizon and control horizon are used in the simulation in order to compare the control performance of the two MPC controllers. The choice of predictive horizon is important. If the predictive horizon is too small, the dynamic range of the system cannot be covered. For example, the overshoot phenomenon occurs in the acceleration and deceleration operating conditions. The predictive horizon should be guaranteed to include this period to avoid overshoot. However, if the predictive horizon is too large, it will increase the amount of computation. Because of the strong nonlinearity of the diesel engine, the controller still has prediction errors even with the compensation of DO. Therefore, the longer the predictive horizon is, the greater the prediction error of the last step in the predictive horizon may lead to deterioration of control performance. It is reasonable to choose the predictive horizon as 15 by the simulation experiment, which is equivalent to predicting the speed of the future 5 revolution. The selection of the control horizon refers to the common range, which is selected as 3, that is, covering the working range of the diesel engine 1 revolution.

In addition, the weighted matrix $\mathbf{\Gamma}_y$ and $\mathbf{\Gamma}_u$ in the objective function are also parameters that need to be determined. The change rate of control variables under the same condition can be changed by adjusting the weighting matrix $\mathbf{\Gamma}_y$ and $\mathbf{\Gamma}_u$. The same weighting matrix is used in the two predictive controllers for comparison.

The simulation results of the two predictive controllers on the cylinder-by-cylinder MVEM are shown in Fig.9 and PID controller is selected for comparison. On the whole, the two MPC controllers have achieved excellent control effect. The speed control performance of the two controllers is similar, both of which are significantly better than the PID controller as expected. The following is a further detailed comparison of several typical operating conditions.

Figure 10 shows the simulation results of the two MPC controllers and PID controller when the output speed is close to the reference value under acceleration and deceleration operating conditions. It can be seen from Fig.10 that the control effects of the two MPC controllers are basically the same. The main reason is that the incremental linear prediction model can compensate the prediction error to some

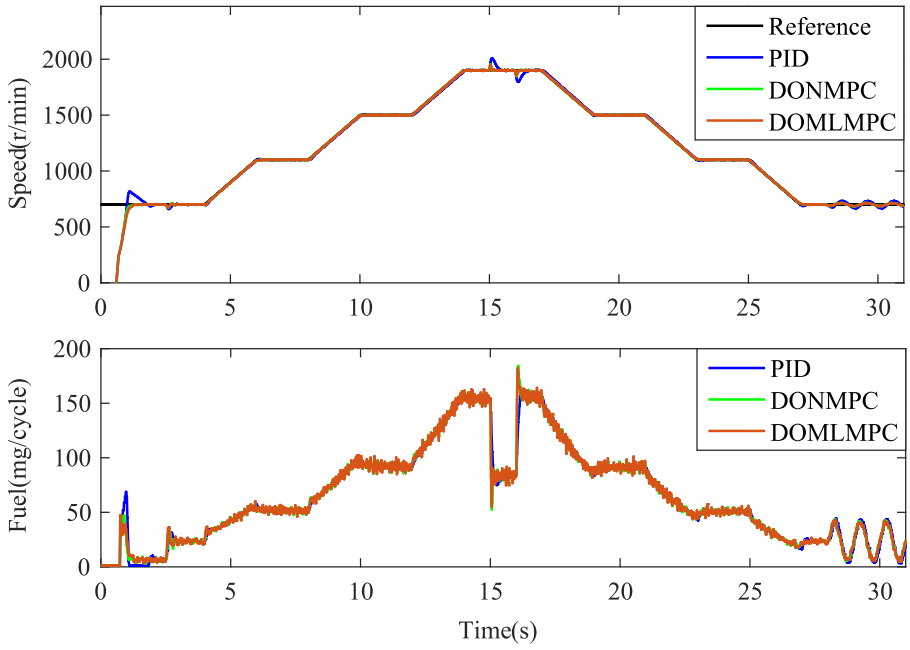

FIGURE 9. Control effect under all operating conditions of software simulation.

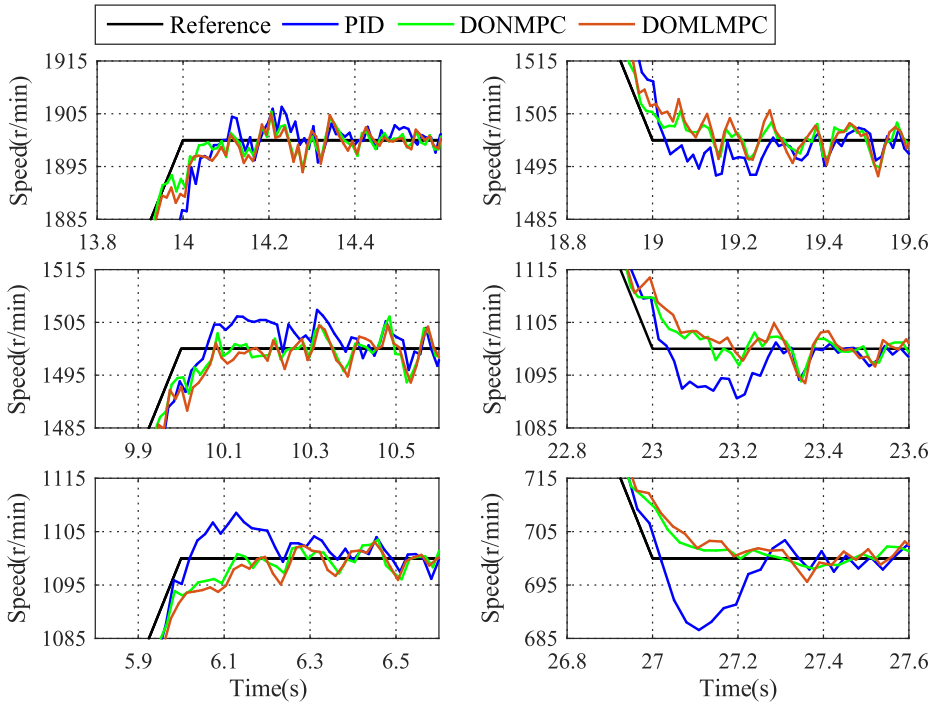

FIGURE 10. Control effect under acceleration and deceleration operating conditions of software simulation.

extent. In addition, each set of parameters $\mathbf{S}_{x,i}$, $\mathbf{S}_{u,i}$ and $\mathbf{S}_{d,i}$ used by the DOLMMPC controller is calculated based on a specific reference speed. For each set of DOLMMPC controller parameters, the error is maximum when the output speed is equal to the median of the two adjacent reference speeds. Because the diesel engine is in the acceleration and deceleration stage at this time, the injection quality of each cycle changes greatly, so the error of the parameters will not

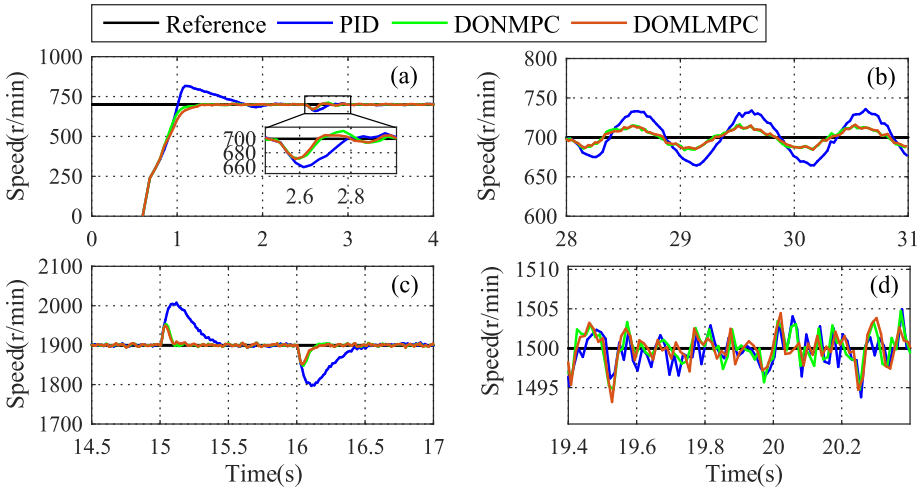

FIGURE 11. Control effect under multiple operating conditions of software simulation.

have a great impact on the output variables. It also shows that the DOLMMPC controller designed in this manuscript can greatly reduce the amount of online computation and does not have a great impact on the control performance. Moreover, the two MPC controllers have achieved good control effect in each acceleration and deceleration process without overshoot, and the control performance is significantly better than that of PID controller.

Figure 11 shows the control effects of two MPC controllers and PID controllers under multiple operating conditions. Subfigure (a) shows that the DONMPC controller and DOLMMPC controller still maintain similar control effects in the starting operating condition and the first loading, and the control effects of the two MPC controllers are respectively better than that of the PID controller. Subfigures (b) and (c) show the control effect of load mutation operating condition and periodic load operating condition respectively. As can be seen from the figures, the control effects of the two MPC controllers are still similar and obviously superior to PID controller. Subfigure (d) shows speed fluctuation effect under steady-state operating condition. As can be seen from the subfigure (d), steady-state fluctuation effects of the three controllers are similar. In conclusion, the performance of the two MPC controllers is better than that of the PID controller in software simulation. In addition, the control effect of the two MPC controllers is similar in most operating conditions, which indicates that the two MPC controllers can be mutually substituted in the premise of ignoring the amount of online calculation.

B. SEMI-PHYSICAL SIMULATION AND ANALYSIS

In this sub-section, the semi-physical simulation experiments are carried out for the designed DOLMMPC controller based on the cylinder-by-cylinder MVEM. The DOLMMPC controller will run in a real ECU, and PID controller is also selected for comparison. The main test operating conditions are the same as those in the software simulation stage, and the same load change value is set.

The composition of the semi-physical simulation platform is shown in Fig.12. The cylinder-by-cylinder MVEM is compiled in the host computer A and generates .dll file. Then, the.dll file is loaded into the real-time host of the HIL cabinet over the local area network to complete the download of the model. The control strategy is generated embedded C code in the host computer B, and downloaded into the ECU through CANape. The ECU used in the experiments is based on the NXP MPC5644A microcontroller, which uses the e200z4 core and has a maximum clock speed of 150MHz. During operation, the HIL cabinet sends magnetoelectric crankshaft sensor signals and camshaft sensor signals to the ECU through the speed signal conditioning board. Thus, ECU can determine the phase of the diesel engine according to position of that the missing teeth of crankshaft gear and the position of that the more tooth of camshaft gear, and calculate the speed in real time according to the crankshaft speed signal. The ECU directly drives the fuel injector through the fuel injection drive circuit, and the fuel injection acquisition channel of the HIL cabinet can capture the fuel injector opening time and apply it to the diesel engine model to form the closed loop. The on-line real-time calibration and monitoring of variables were completed by CANape.

The experimental results of acceleration and deceleration operating conditions are shown in Fig.13. It can be seen from the figure that the DOLMMPC controller designed still has better dynamic performance than PID controller when running in real microprocessor. By comparison with Fig.10, it can be found that the control performance shown in acceleration and deceleration operating conditions does not change much compared with the software simulation no matter DOMLMPC controller or PID controller. The overshoot or convergence time of the PID controller has a small increase only when the steady state is reached. The main reason is

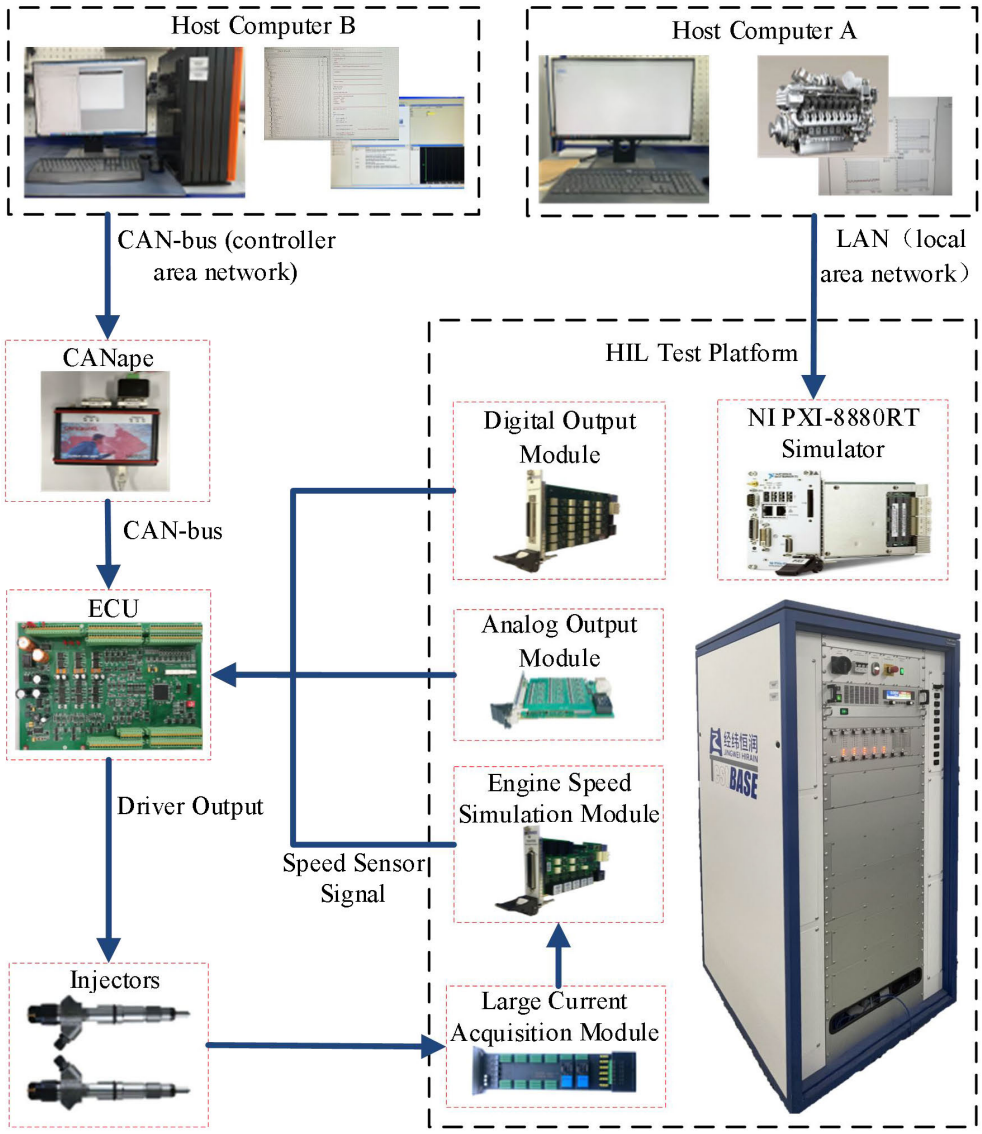

FIGURE 12. The composition of the semi-physical simulation platform.

that there will be a delay in the acquisition of fuel injection duration and output speed signal of the signal conditioning board, resulting in a small slowdown in the response speed of the control process in the semi-physical simulation. The control effect of DOLMMPC controller is similar to that of software simulation. There is no overshoot due to signal delay, and the convergence time is shorter than that of PID controller.

The experimental results under multiple operating conditions are shown in Fig.14. In the starting operating condition of the subfigure (a), the control effect of the PID controller changes greatly, there is a larger overshoot than that of the software simulation, and the convergence time is increased. However, consistent with the above analysis, there is basically no overshoot in results of the DOLMMPC controller due to the rolling optimization. The DOLMMPC controller is still less disturbed than the PID controller at the first load. This situation is also shown in subfigure (b) and subfigure (c). DOLMMPC controller shows far better performance than PID controller no matter in load mutation operating condition or periodic load operating condition. In the subfigure (d), the steady-state fluctuation of the two controllers is basically the same. Only due to the existence of delay and extra noise in the semi-physical simulation experiments, the steady-state fluctuation is increased compared with that of the software simulation. But it still meets the requirement of speed control precision.

The semi-physical simulation results show that the designed DOLMMPC controller can be applied to ECU. The comparison between DOLMMPC controller and PID controller shows that the performance of DOMLMPC controller is much better than PID controller in acceleration and

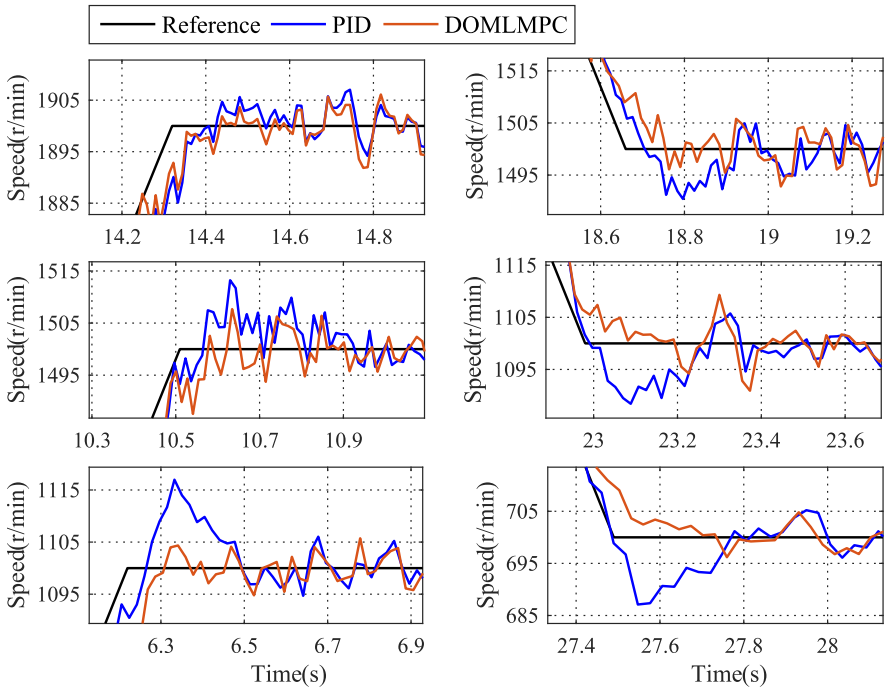

FIGURE 13. Control effect under acceleration and deceleration operating conditions of semi-physical simulation.

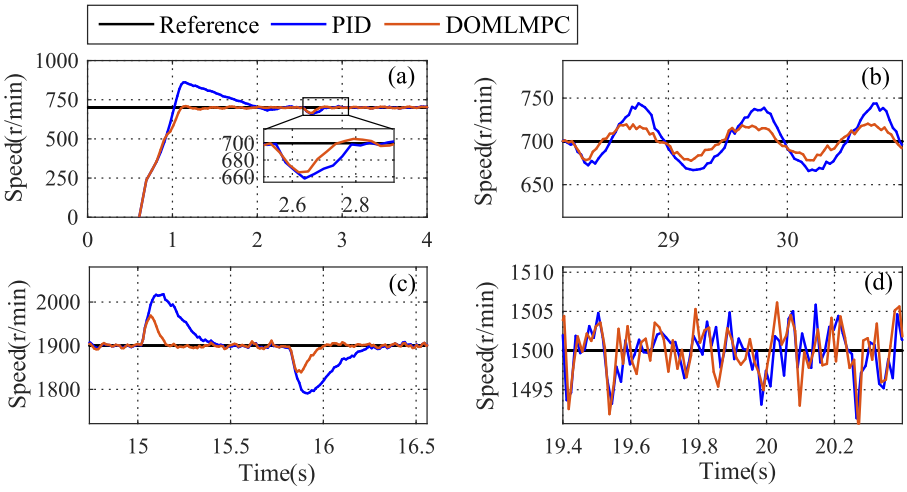

FIGURE 14. Control effect under multiple operating conditions of semi-physical simulation.

deceleration operating conditions, starting operating condition, periodic load operating condition and load mutation operating condition. In the steady-state operating condition, the steady-state fluctuation of the two controllers is basically the same. The above advantages are consistent with those of software simulation. In addition, when facing the delay of signal acquisition and control output in acceleration and deceleration operating conditions, DOMLMPC controller still has no overshoot due to the effect of off-line rolling optimization.

V. CONCLUSION

In order to improve the speed control performance of marine diesel engine, the MPC algorithm is introduced into the speed controller, and the optimization design of the MPC controller is carried out on the premise of simplifying the calculation without sacrificing the control performance greatly. Firstly, in view of the problem that conventional MPC controllers are prone to steady-state errors, an MPC controller based on incremental nonlinear prediction model is proposed. And referring to [4], the discrete DO is introduced in the feedback

correction of the MPC controller. The requirement of MPC controller for the accuracy of prediction model is reduced by using the mentioned DO. Meanwhile, because of the filtering effect of the DO itself, the influence of high frequency disturbance in the feedback on the control performance is weakened. Then, the calculation of the designed controller is simplified. The nonlinear model used for algorithm design is transformed into linear model, and it is constructed as an incremental form. However, the calculation amount is still difficult to meet the demand of diesel ECU. Therefore, a DOLMMPC controller which can calculate parameters off-line is proposed. The analysis shows that the DOLMMPC controller is less computative, so it should be able to run in real time in diesel ECU, and has similar control performance to the DONMPC controller. In order to verify the above analysis, a cylinder-by-cylinder MVEM is built based on the MVEM, which is closer to the actual operation of the diesel engine. And the software simulation experiments of proposed MPC controllers and PID controller are carried out based on the cylinder-by-cylinder MVEM. The experimental results show that the performance of the two MPC controllers is similar, and both of them are better than PID controllers. Then, the DOLMMPC controller and PID controller are verified on the semi-physical simulation platform. The experimental results demonstrate that the DOLMMPC controller can run in diesel ECU and has the same advantages as that of the software simulation. In conclusion, the DOLMMPC controller designed in this manuscript can be used in practical engineering to improve the performance of diesel engine speed control.

ACKNOWLEDGMENT

The authors would like to thank the Editor-in-Chief, an Associate Editor, and anonymous referees for their invaluable comments and suggestions.

REFERENCES

[1] R. Wang, X. Li, Y. Liu, W. Fu, S. Liu, and X. Ma, "Multiple model predictive functional control for marine diesel engine," *Math. Problems Eng.*, vol. 2018, May 2018, Art. no. 3252653, doi: 10.1155/2018/3252653.

[2] Y. Yuan, M. Zhang, Y. Chen, and X. Mao, "Multi-sliding surface control for the speed regulation system of ship diesel engines," *Trans. Inst. Meas. Control*, vol. 40, no. 1, pp. 22–34, Jan. 2018, doi: 10.1177/0142331216649022.

[3] Y. Hu, J. Yang, N. Hu, L. Hu, Z. Qian, and Y. Yu, "Research and development of electronic speed control strategies for medium-speed marine diesel engines," *Int. J. Engine Res.*, vol. 19, no. 5, pp. 584–596, Jun. 2018, doi: 10.1177/1468087417725005.

[4] X. Li, Y. Liu, H. Shu, R. Wang, Y. Yang, and C. Feng, "Disturbance observer-based discrete sliding-mode control for a marine diesel engine with variable sampling control technique," *J. Control Sci. Eng.*, vol. 2020, Jul. 2020, Art. no. 2456850.

[5] D. E. Winterbone and S. Jai-In, "The application of modern control theory to a turbocharged diesel engine powerplant," *Proc. Inst. Mech. Eng. I, J. Syst. Control Eng.*, vol. 205, no. 1, pp. 69–83, Feb. 1991. [Online]. Available: https://journals.sagepub.com/doi/abs/10.1243/pime_proc_1991_205_314_02, doi: 10.1243/PIME_PROC_1991_205_314_02.

[6] X. Li, Q. Ahmed, and G. Rizzoni, "Nonlinear robust control of marine diesel engine," *J. Mar. Eng. Technol.*, vol. 16, no. 1, pp. 1–10, Jan. 2017, doi: 10.1080/20464177.2016.1254455.

[7] X. Shen and Y. Su, "Marine diesel engine speed control system based on fuzzy-PID," in *Proc. Int. Conf. Mech. Eng. Mater.*, Melbourne, VIC, Australia, Jan. 2012, pp. 1589–1594.

[8] Y. Li, Z. Yao, and Y. Xu, "Study on fuzzy-PID control simulation of diesel engines electronic governor," in *Proc. Int. Conf. Process Equip., Mechatronics Eng. Mater. Sci.*, Wuhan, China, Jun. 2013, pp. 263–266.

[9] F. A. Mohamed and H. N. Koivo, "Diesel engine systems with genetic algorithm self tuning PID controller," Presented at the Int. Conf. Future Power Syst., Amsterdam, The Netherlands, Nov. 2005.

[10] H. Fang, L. Chen, and Z. Shen, "Application of an improved PSO algorithm to optimal tuning of PID gains for water turbine governor," *Energy Convers. Manage.*, vol. 52, no. 4, pp. 1763–1770, Apr. 2011, doi: 10.1016/j.enconman.2010.11.005.

[11] W. Meng and C. Guo, "Research on speed intelligent control based on neural networks for large marine main diesel engine," in *Proc. 8th World Congr. Intell. Control Autom.*, Jinan, China, Jul. 2010, pp. 4667–4670.

[12] H.-C. Chen, "Optimal fuzzy PID controller design for an active magnetic bearing system based on adaptive genetic algorithms," *Math. Struct. Comput. Sci.*, vol. 24, no. 5, Oct. 2014, Art. no. e240516.

[13] B. Duan, T. Sun, Z. Li, and G. Mei, "Expert adaptive ANN-PID control in digital invert power supply," in *Proc. IEEE Int. Conf. Autom. Logistics*, Shenyang, China, Aug. 2009, pp. 1268–1272.

[14] S. Dadvandipour, N. Khalili Dizaji, and S. Rosshan Entezar, "An approach to optimize the proportional-integral-derivative controller system," in *Proc. 16th Int. Carpathian Control Conf. (ICCC)*, Szilvásvárad, Hungary, May 2015, pp. 95–99.

[15] R. Wang, X. Li, J. Zhang, J. Zhang, W. Li, Y. Liu, W. Fu, and X. Ma, "Speed control for a marine diesel engine based on the combined linear-nonlinear active disturbance rejection control," *Math. Problems Eng.*, vol. 2018, Dec. 2018, Art. no. 7641862.

[16] R. Wang, X. Li, Y. Liu, Q. Ahemd, Y. Yang, C. Feng, and X. Ma, "Variable sampling rate based active disturbance control for a marine diesel engine," *Electronics*, vol. 8, no. 4, p. 370, Mar. 2019, doi: 10.3390/electronics8040370.

[17] Z. Ju and C. Xinyan, "Explicit model predictive control of 3-DOF helicopter," in *Proc. 26th Chin. Control Decis. Conf. (CCDC)*, Changsha, China, May/Jun. 2014, pp. 3083–3088.

[18] H.-B. Kuntze, A. Jacubasch, J. Richalet, and C. Arber, "On the predictive functional control of an elastic industrial robot," in *Proc. 25th IEEE Conf. Decis. Control*, Athens, Greece, Dec. 1986, pp. 1877–1881.

[19] A. Bemporad, M. Morari, V. Dua, and E. N. Pistikopoulos, "The explicit linear quadratic regulator for constrained systems," *Automatica*, vol. 38, no. 1, pp. 3–20, Jan. 2002. [Online]. Available: https://www.sciencedirect.com/science/article/pii/S0005109803001900, doi: 10.1016/S0005-1098(01)00174-1.

[20] J. Zhang and X. Xiu, "*K*-d tree based approach for point location problem in explicit model predictive control," *J. Franklin Inst., Eng. Appl. Math.*, vol. 355, no. 13, pp. 5431–5451, Sep. 2018, doi: 10.1016/j.jfranklin.2018.05.040.

[21] X. Qian, Y. Yin, X. Zhang, X. Sun, and H. Shen, "Model predictive controller using Laguerre functions for dynamic positioning system," in *Proc. 35th Chin. Control Conf. (CCC)*, Chengdu, China, Jul. 2016, pp. 4436–4441.

[22] F. Xu, H. Chen, X. Gong, and Q. Mei, "Fast nonlinear model predictive control on FPGA using particle swarm optimization," *IEEE Trans. Ind. Electron.*, vol. 63, no. 1, pp. 310–321, Jan. 2016, doi: 10.1109/TIE.2015.2464171.

[23] J. Chang and Y. Peng, "Nonlinear Francis hydroturbine generator set neural network model predict control," in *Proc. 5th Int. Conf. Mach. Learn. Cybern.*, Dalian, China, Aug. 2006, pp. 2963–2968.

[24] H. Zhang, J. Yan, W. Wang, M. Xu, and W. Ma, "Self-tuning predictive control applicable to ship magnetic levitation damping device," *IET Collaborative Intell. Manuf.*, vol. 4, no. 1, pp. 58–70, Mar. 2022. [Online]. Available: https://ietresearch.onlinelibrary.wiley.com/doi/10.1049/cim2.12044, doi: 10.1049/cim2.12044.

[25] D. Dougherty and D. Cooper, "A practical multiple model adaptive strategy for single-loop MPC," *Control Eng. Pract.*, vol. 11, no. 2, pp. 141–159, Feb. 2003.

[26] X. Tao, N. Li, and S. Li, "Multiple model predictive control for large envelope flight of hypersonic vehicle systems," *Inf. Sci.*, vol. 328, pp. 115–126, Jan. 2016, doi: 10.1016/j.ins.2015.08.033.

[27] H. Yu, J. Duan, S. Taheri, H. Cheng, and Z. Qi, "A model predictive control approach combined unscented Kalman filter vehicle state estimation in intelligent vehicle trajectory tracking," *Adv. Mech. Eng.*, vol. 7, no. 5, May 2015, Art. no. 168781401557836.

[28] Y. Liu, S. Cheng, B. Ning, and Y. Li, "Robust model predictive control with simplified repetitive control for electrical machine drives," *IEEE Trans. Power Electron.*, vol. 34, no. 5, pp. 4524–4535, May 2019, doi: 10.1109/TPEL.2018.2857837.
[29] Á. J. Prado, M. Torres-Torriti, J. Yuz, and F. A. Cheein, "Tube-based nonlinear model predictive control for autonomous skid-steer mobile robots with tire–terrain interactions," *Control Eng. Pract.*, vol. 101, Aug. 2020, Art. no. 104451.
[30] Z. Cai, H. Zhou, J. Zhao, K. Wu, and Y. Wang, "Formation control of multiple unmanned aerial vehicles by event-triggered distributed model predictive control," *IEEE Access*, vol. 6, pp. 55614–55627, 2018. [Online]. Available: https://ieeexplore.ieee.org/document/8478208, doi: 10.1109/ACCESS.2018.2872529.
[31] S. Li, Z. Li, Z. Yu, B. Zhang, and N. Zhang, "Dynamic trajectory planning and tracking for autonomous vehicle with obstacle avoidance based on model predictive control," *IEEE Access*, vol. 7, pp. 132074–132086, 2019. [Online]. Available: https://ieeexplore.ieee.org/document/8835033, doi: 10.1109/ACCESS.2019.2940758.
[32] A. Murilo, M. Alamir, and D. Alberer, "A general NMPC framework for a diesel engine air path," *Int. J. Control*, vol. 87, no. 10, pp. 2194–2207, 2014, doi: 10.1080/00207179.2014.905708.
[33] E. R. Gelso and J. Lindberg, "Air-path model predictive control of a heavy-duty diesel engine with variable valve actuation," in *Proc. IFAC*, Cape Town, South Africa, Aug. 2014, pp. 3012–3017.
[34] M. Keller, S. Geiger, M. Günther, S. Pischinger, D. Abel, and T. Albin, "Model predictive air path control for a two-stage turbocharged spark-ignition engine with low pressure exhaust gas recirculation," *Int. J. Engine Res.*, vol. 21, no. 10, Dec. 2020, Art. no. 1468087420936398.
[35] M. Karlsson, K. Ekholm, P. Strandh, R. Johansson, and P. Tunestål, "Multiple-input multiple-output model predictive control of a diesel engine," *IFAC Proc. Volumes*, vol. 43, no. 7, pp. 131–136, 2010.
[36] B. R. Andrievsky and I. B. Furtat, "Disturbance observers: Methods and applications. I. methods," *Autom. Remote Control*, vol. 81, no. 9, pp. 1563–1610, Sep. 2020, doi: 10.1134/S0005117920090015.
[37] A. Yar, A. I. Bhatti, and Q. Ahmed, "First principle based control oriented model of a gasoline engine including multi-cylinder dynamics," *Control Eng. Pract.*, vol. 70, pp. 63–76, Jan. 2018, doi: 10.1016/j.conengprac.2017.09.020.
[38] E. Hendricks, "A compact, comprehensive model of large turbocharged, two-stroke diesel engines," Presented at the Int. Off-Highway Powerplant Congr. Expo., Milwaukee, WI, USA, Sep. 1986.
[39] J. W. Chung, N. H. Kim, D. J. Kim, and S. S. Jang, "Mean value WGT diesel engine calibration model for effective simulation research," *Int. J. Automot. Technol.*, vol. 19, no. 2, pp. 209–220, Apr. 2018, doi: 10.1007/s12239-018-0020-5.
[40] W. Sui and C. M. Hall, "Control-oriented modeling of combustion phasing on diesel engines," in *Proc. Annu. Amer. Control Conf. (ACC)*, Milwaukee, WI, USA, Jun. 2018, pp. 1616–1621.
[41] S. Loganathan, R. Murali Manohar, R. Thamaraikannan, R. Dhanasekaran, A. Rameshbabu, and V. Krishnamoorthy, "Direct injection diesel engine rate of heat release prediction using universal load correction factor in double Wiebe function for performance simulation," Presented at the SAE Tech. Paper. [Online]. Available: https://saemobilus.sae.org/content/2011-01-2456/
[42] X. Li, Y. Liu, J. Zhang, and R. Wang, "Disturbance observer-based finite-time speed control for marine diesel engine with input constraints," *IEEE Access*, vol. 8, pp. 50859–50871, 2020. [Online]. Available: https:// ieeexplore.ieee.org/document/9034076/, doi: 10.1109/ACCESS.2020.2980371.
[43] J. Han, "Invariability of time optimal feedback control," *J. Syst. Sci. Math Sci.*, vol. 25, no. 4, pp. 116–124, Aug. 2005.
[44] J. Q. Han, "From PID technique to active disturbances rejection control technique," *Control Eng. China*, vol. 9, no. 3, pp. 13–18, May 2002.

HAOYU SHU was born in Jilin, China, in 1997. He received the B.S. degree in thermal energy and power engineering from Northeast Petroleum University, in 2019. He is currently pursuing the Ph.D. degree in power engineering and engineering thermo-physics with the College of Power and Energy Engineering, Harbin Engineering University.

His research interests include the application of intelligent algorithm in diesel engine, including model predictive control, active disturbance rejection control, and sliding mode control.

XUEMIN LI received the Graduate degree in internal combustion engine from Southwest Jiaotong University, in 1994, and the M.S. and Ph.D. degrees in internal combustion engine from Jilin University, in 2002 and 2005, respectively.

In 2005, he joined the College of Power and Energy Engineering, Harbin Engineering University, where he was an Assistant Professor in marine diesel control. In August 2013, he was appointed as a Professor in power mechanical and engineering with Harbin Engineering University. His research interests include the electronic control of internal engines, including the application of intelligent control technology, the fuel injection technology of diesel engine, and embedded system design.

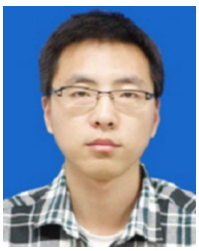

YUFEI LIU was born in Henan, China, in 1990. He received the B.S. degree in thermal energy and power engineering and the M.S. and Ph.D. degrees from Harbin Engineering University, Harbin, China, in 2012, 2014, and 2022, respectively.

He is currently an Engineer with Jingwei Hirain Company, Beijing. His research interests include vehicle control strategy and related control algorithms, including sliding mode control, fuzzy control, and active disturbance rejection control.

RUNZHI WANG was born in Hengyang, China, in 1990. He received the B.S. degree in thermal energy and power engineering and the Ph.D. degree from Harbin Engineering University, in 2013 and 2022, respectively.

He is currently a Lecturer with the School of Mechanical and Electrical Engineering, Suqian University. His research interests include the application of intelligent algorithm in diesel engines and electric motors, he also does study in model predictive control, active disturbance rejection control, and sliding mode control.